



Synthesis, Characterization and Thermal Analysis of Cu (II), Co (II), Ru(III) and Rh(III) Complexes of a New Acidic Ligand

Rasha Khider Hussain Al-Daffay *✉

Department of Chemistry, College of Science,
University of Baghdad, Baghdad, Iraq.

Abbas Ali Salih Al-Hamdani ✉

Department of Chemistry, College of Sciences for
Women, University of Baghdad, Baghdad, Iraq.

Wail Al Zoubi ✉

School of Materials Science and Engineering,
Yeungnam University, Gyeongsan 712-749, South
Korea.

*Corresponding Author: rasha.khodair1105a@cs.w.uobaghdad.edu.iq

Article history: Received 28 September 2022, Accepted 27 December 2022, Published in October 2023.

doi.org/10.30526/36.4.3047

Abstract

Hippuric acid and 3-amino phenol were used to make the 4-(2-Amino-4-hydroxy-phenylazo)-benzoylamino-acetic acid diazonium salt, a new Azo molecule that is a derivative of the (4-Amino-benzoylamino)-acetic acid diazonium salt. We found out what the ligand's chemical structures were by using information from ¹HNMR, FTIR, CHN, UV-Vis, LC-mass spectroscopy, and thermal analyses. To make metal complexes of the azo ligand with Co(II), Cu(II), Ru(III), and Rh(III) ions, extra amounts of each azo ligand were mixed with metal chloride salts in a 2:2 mole ratio. The stereochemical structures and geometries of the metal complexes that were studied were guessed based on the fact that the ligand exhibited tetradentate bonding behavior when combined with the metal ions. The azodye ligand is coordinated with the metal ions (Co(II), Cu(II), Ru(III), and Rh(III)) through (NNOO) the N atoms of azo and amine groups and the oxygen of carboxylic and phenolic hydroxyl groups. According to analytical results, the Ru(III) and Rh(III) complexes have binuclear octahedral geometry, whereas the Cu(II) and Co(II) complexes have binuclear distorted octahedral and binuclear tetrahedral geometry, respectively. The results indicated that the following formulas for ligand complexes should be used: [Ru₂Cl₂(H₂O)₂(LI)₂], [Rh₂Cl₂(H₂O)₂(LI)₂], [Co₂(LI)₂], and [Cu₂(LI)₂]. The thermal analysis conducted by TG, DTG, and DTA demonstrated partial breakdown at temperatures between 820°C and 850°C.



Keywords: Azo ligand (acidic), Mass spectroscopy, Metal complexes, TGA.

1. Introduction

Azo compounds are among the earliest organic molecules ever synthesized, and the dye industry still makes extensive use of them. A class of chemical compounds known as azo dyes has at least one azochromophore (R1-N=N-R2), which gives these well-known dyes their hue. They are crucial to both scholarly and practical research. [2,3] The functional group (-N=N-) that joins two symmetric, asymmetric, identical, or non-azo alkyl or aryl radicals is what sets these molecules apart. [3] The fundamental method of synthetic synthesis is based on Peter Griess's nineteenth-century discovery of the diazotization reaction. [2] An aromatic primary amine is diazotized to make most of the azo dyes. These dyes then join with one or more electron-rich nucleophiles, such as amino or hydroxyl [4,5]. As a result of their many benefits, which include antibacterial and antifungal agents, dyeing procedures, photoelectronics, and sensitizers in photocatalytic reactions, Because of their numerous benefits, including their use as antibacterial and antifungal agents, dyeing processes, photoelectronics, and sensitizers in photocatalytic reactions, azo compounds, particularly aromatic type 1, are recognized as important organic chemicals [3]. The most prevalent applications are in textile dyeing procedures, paper printing, color photography, pharmaceuticals, food, cosmetics, leathers, edibles, medication additives, plastics, and paints. In addition to serving as a colorant, they also have biological effects such as antimicrobial, antifungal, cytotoxic, and antiproliferative qualities. Additionally, in addition to serving as beneficial colorants and antibacterial agents, synthetic azo compounds are now an important part of many medical tests [4, 6-8].

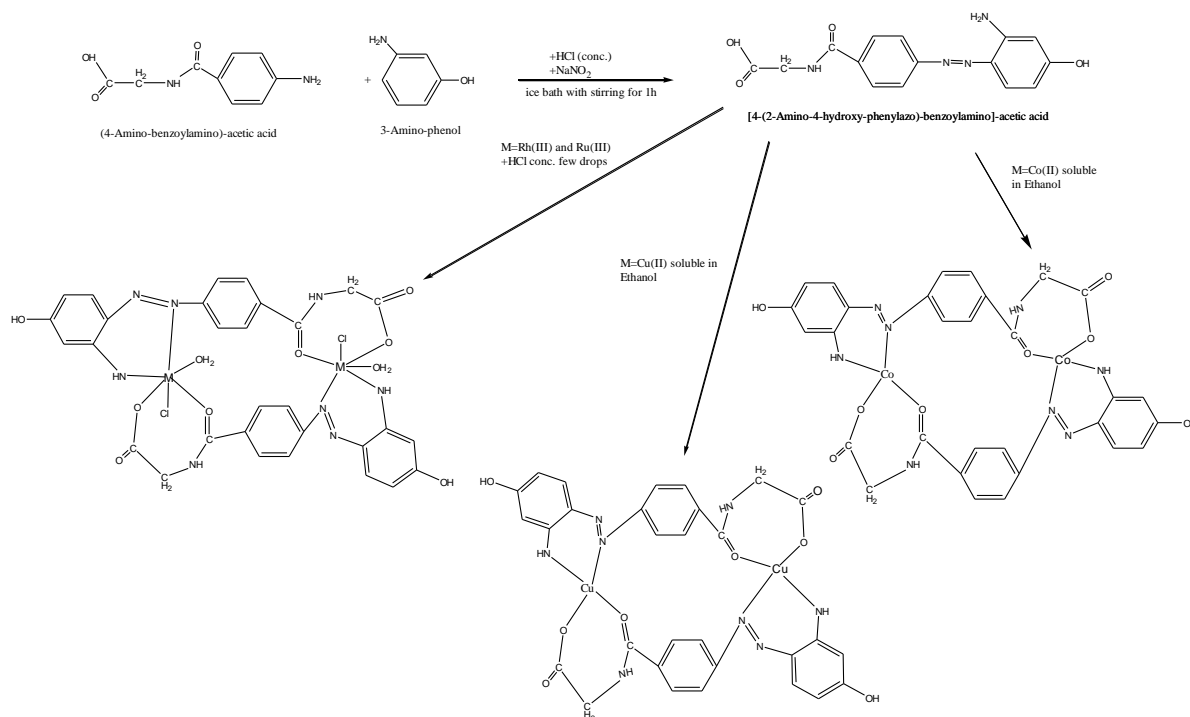
2. Experimental

2.1. Materials and apparatus:

Sigma-Aldrich, Merck, and other retailers provided all the chemicals and reagents, which were used exactly as provided. For the elemental study, the vector model 3000/EA. 3-single was employed (C, H, and N). Using the gravimetric approach, metal ions were calculated as metal oxides. The molar conductivity of the complexes was determined by using the conductometer WTW at room temperature and 1103 M conc. All the complexes were dissolved in dimethylformamide (DMF). QP50A: DI Using mass spectrometry (MS), For numerous different compounds, mass spectra were collected using a Shimadzu QP-2010-Plus (E170Ev) spectrometer. The spectrum was analyzed using the UV-Vis spectrophotometer Shimadzu 1800, and the proton-nuclear magnetic resonance (Proton-NMR) spectrum for the ligand in DMSO-d₆ was captured using a Bruker 400 MHz. In order to analyze Fourier transform infrared (FTIR) spectra, the IR Prestige-21 was employed, while thermogravimetric research was conducted using a PerkinElmer PyrisDiamond TGA.

2.2. Synthesis of azo dye ligand 4-(2-Amino-4-hydroxy-phenylazo)-benzoyl amino-acetic acid

P-amino hippuric acid (0.194 g, 1 mmole) was heated to 5 °C with a 10% solution of NaNO₂ and melted in a mixture of 5 ml ethanol and 3 ml HCl. To create 3-aminophenol, a cooled ethanolic solution was combined with a diazotized solution (0.109g, 1mmole). The result of this direct mixing was a murky-colored mixture with azo ligand precipitation, then filtered and washed with a (1:1) (C₂H₅OH:H₂O) solution for a number of ounces, and then dried. Scheme 1 illustrates the response.



Scheme 1. Azo dye synthesised and its complexes

2.3. Typical procedure for creating complexes of metallic ions

Stoichiometric amounts of (0.364, 1 m.mol) and (0.357, 1 m.mol) of [2:2] M:L for Cu II and Co II chloride salts, respectively, were added to azo ligand that was dissolved (0.280g, 1 m.mol) in 10 mL of pure ethanol while stirring. The same amounts of ligand were also added to the Cu(II) and Co(II) (0.311, 1 m.mol). All of the complexes were combined and heated to 65°C for two hours. After cooling in an ice bath until precipitation, the mixture was left to chill overnight. In **Scheme 1**, the reaction is displayed. The solid complexes were separated and then rinsed with distilled water and a touch of hot ethanol to remove any unreacted components. We used vacuum desiccators to dry the compounds. An overview of the ligand's analytical, physical, and metal complex properties can be found in **Table 1**.

3. Result & discussion

3.1. The ligand's physical and molecular characteristics

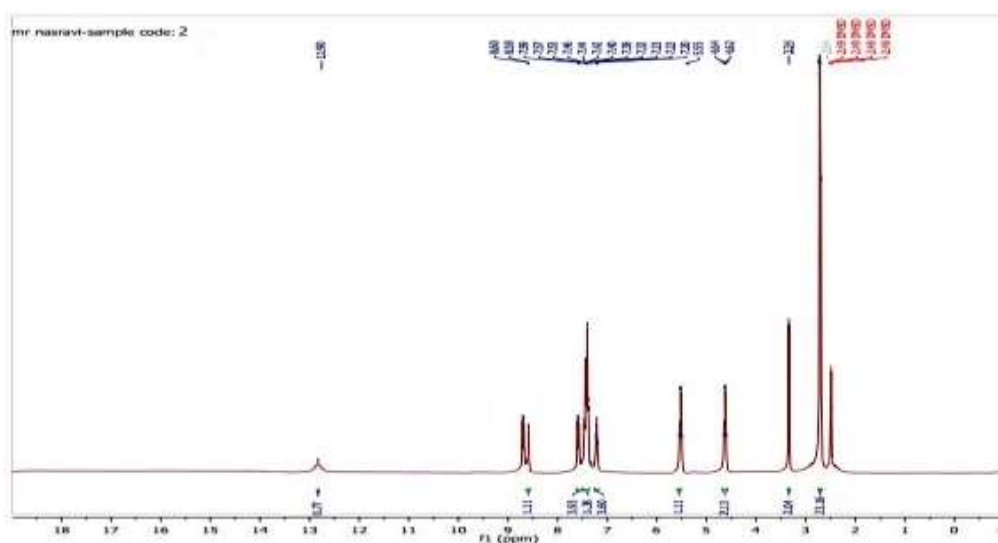
The azo dye ligand (LH₂) resembles a fine brown powder and has an amorphous look. This synthesis ligand is sparingly soluble in ethanol, but it is soluble in water and DMSO. The metallic ion and azoligand complexes were stable in the presence of air.

Table 1. Physical characteristics and analytical information regarding ligands and their compounds.

Comps	ChemicalFormula MolecularWeight g.mol ⁻¹	Colour	Meltin g point	Elemental Compositions%				
				C Founde d (Calc)	H Founde d (Calc)	N Founde d (Calc)	O Founde d (Calc)	M Founde d (Calc)
LH ₂	C ₁₅ H ₁₄ N ₄ O ₄ 314	Brown	280	56.51 (57.32)	3.41 (4.46)	18.71 (17.83)	21.29 (20.38)	-
[Cu ₂ L ₂]	C ₃₀ H ₂₄ N ₈ O ₈ Cu ₂ 751	Light green	285	46.55 (47.93)	4.33 (3.2)	16.05 (14.91)	16.01 (17.07)	15.83 (16.91)
[Co ₂ L ₂]	C ₃₀ H ₂₄ N ₈ O ₈ Co ₂ 742	Dark green	290	46.99 (48.52)	4.05 (3.23)	16.55 (15.09)	18.01 (17.25)	16.83 (15.90)
[Rh ₂ L ₂ Cl ₂ (H ₂ O) ₂]	C ₃₀ H ₂₈ N ₈ O ₁₀ Rh ₂ Cl ₂ 937	Deep Brown	297	36.96 (38.42)	2.22 (2.99)	12.61 (11.95)	18.10 (17.08)	-
[Ru ₂ L ₂ Cl ₂ (H ₂ O) ₂]	C ₃₀ H ₂₈ N ₈ O ₁₀ Ru ₂ Cl ₂ 933	Deep Brown	296	39.93 (38.59)	2.90 (3.00)	13.12 (12.0)	16.16 (17.15)	-

3.2. ¹H-NMR spectra

The ligand's ¹H-NMR spectrum showed a peak at 5.55 ppm, and it was found that the chemical shifts of phenolic OH were to blame. The triplet peaks at 8.6 ppm were given the secondary (NH) proton's chemical shift on the spectrum. The CH₂-COO proton was identified as the source of the numerous signals detected at 3.3 ppm for the ligand. At 4.64 ppm, the primary amine group first appears as a singlet. The aromatic protons of benzene groups are thought to be responsible for the several peaks at 6.82–7.56 ppm. The protonOH of the carboxyl group COOH is what causes the singlet signal at 12.9 ppm. [9, 10]

**Figure1.** H-NR spectrumof azo ligand

3.3. Electronic spectra measurements

The UV-Vis spectra of the ligand LH2 and Co(II) complex are displayed in **Table 2** and **Figure 2a**. The (N=N) azogroup's n^* transition in the free ligand caused two peaks at 402 and 421-445 [11]. The (N=N) azogroup's n^* transition in the free ligand also caused a peak with an absorption maximum at 402 [11]. These peaks were displaced in the spectra of all metal complexes, proving that the coordination process involves the azo group [12]. The spectrum of the Co(II) complex contained three bands at 250, 441, and 890 nm attributed to the ligand field and charge transfer. ${}^4A_{2(F)} \rightarrow {}^4T_{1(P)}$ and ${}^4A_{2(F)} \rightarrow {}^4T_{2(F)}$ transitions, respectively assigned to the tetrahedral Co(II) ion, which is indicative of a tetrahedral geometry (**Figure 2b**). The electronic spectrum of the Cu(II) complex displays one new absorption peak. The peak at 953 nm is caused by (d-d) spinallowed electronic transitions of type ${}^2B_{1g} \rightarrow {}^2A_{1g}$, and its location and width are caused by the JahnTeller effect, which works on the d^9 electronic ground state of six coordinated systems. These properties are strong indicators of distorted octahedral geometry [13]. The octahedral geometry of the Rh(III) complex can be attributed to bands in the electronic spectra at 24752, (23585-22075) cm^{-1} , and 10482 cm^{-1} , which have been assigned to ${}^1A_{1g} \rightarrow {}^1T_{1g}$ and ${}^1A_{1g} \rightarrow {}^1T_{2g}$ transitions, respectively. [14] As a Ru(III) complex, it showed three spectral lines at 253, 401, and 418–449 nm. Band 2 is attributed to the LMCT transition, and band 3 corresponds to the ${}^2T_{2g} \rightarrow {}^2A_{2g}$ [15] transition. The UV-vis examination also revealed the emergence of metal (II) and (III) azodye complexes. The electronic spectra of the created azodye ligand and its metal complexes in DMSO solutions (1×10^{-3} M) span from 200 to 1100 nm [9, 16].

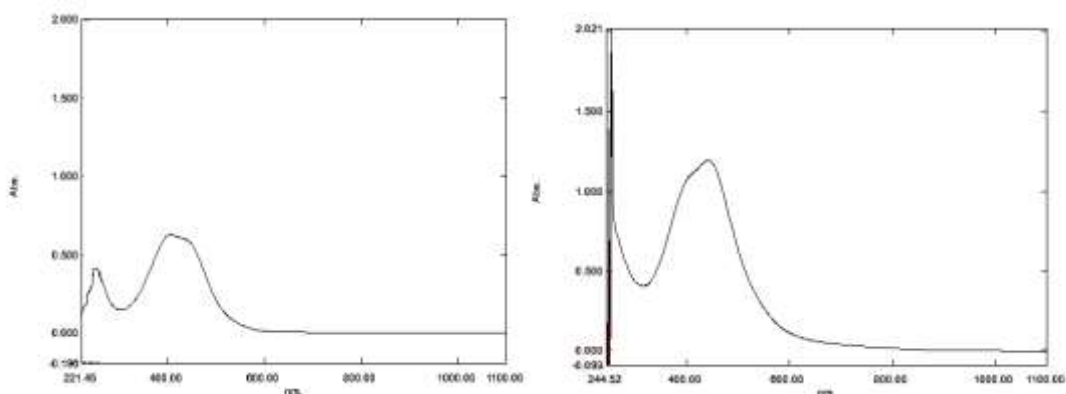


Figure 2. a- Electronic spectra of azo ligand b- Electronic spectra of Co(II) complex

Table 2. Electronic information and molar conductivity for metal complexes in DMSO with the LH₂ ligand (0.001 M)

Geometry of Complexes	λ_{\max} (nm)	$\nu_{\text{cm}^{-1}}$	ABS	$\epsilon_{\max} \text{ L mol}^{-1} \text{ cm}^{-1}$	Assignment	$\Lambda_{\text{m}} \text{ cm}^2 \Omega^{-1} \text{ mol}^{-1}$
LH ₂	260	38462	0.248	248	$\pi \rightarrow \pi^*$	-
	402	24876	0.235	235	$n \rightarrow \pi^*$	
	421-445	23753-22472	0.204	204	$n \rightarrow \pi^*$	
[Co ₂ L ₂]	250	40000	1.17	1170	$\pi \rightarrow \pi^*$	20
	441	22676	0.477	477	C.T.	
Tetrahedral	890	11236	0.26	260	${}^4\text{A}_{2(\text{F})} \rightarrow {}^4\text{T}_{1(\text{P})}$	
[Cu ₂ L ₂] Distorted octahedral	277	36101	2.377	2377	$\pi \rightarrow \pi^*$	18
	443	22573	0.055	55	C.T.	
	953	11350			${}^2\text{B}_{1\text{g}} \rightarrow {}^2\text{A}_{1\text{g}}$	
[Ru ₂ L ₂] Octahedral	253	39526	0.102	102	$\pi \rightarrow \pi^*$	17
	401	24938	0.111	111	C.T.	
	(418-449)	23923-22272	0.112	112	${}^2\text{T}_{2\text{g}} \rightarrow {}^2\text{A}_{2\text{g}}$	
[Rh ₂ L ₂] Octahedral	251	39841	0.310	310	$\pi \rightarrow \pi^*$	9
	404	24752	0.280	280	$n \rightarrow \pi^*$	
	(424-453)	23585-22075	0.229	229	${}^1\text{A}_{1\text{g}} \rightarrow {}^1\text{T}_{1\text{g}}$	
	954	10482	0.191	191	${}^1\text{A}_{1\text{g}} \rightarrow {}^1\text{T}_{2\text{g}}$	

3.4. Measurements using liquid chromatography mass spectrometry (LC/MS)

In order to get the mass spectra of the novel ligand-metal complexes, electron impact fragmentation was utilized. In general, substantial fragments linked to breakdown products as well as the free azo ligand and its complexes were found using high-resolution MS. The electron impact mass spectrum of the ligand LH₂ is shown in **Figure 3**. The computed molecular weight of this ligand is 314 g/mol. The signal at 315.30 m/z in the spectra was attributed to a new azo moiety, [C₁₅H₁₅N₃O₃]⁺. Different pieces may be responsible for more unique peaks at 121, 104, and 90 m/z. Their intensity reveals the shards' stability [17]. The mass spectrum of the Cu(II) complex is shown in **Figure 4**. The complex moiety [C₃₀H₂₅N₈O₈Cu₂]⁺ was identified in the spectra as a peak at 751 m/z. Different components may be responsible for two additional unique peaks at 242.68 and 149 m/z. The Co(II) complex's mass spectrum is shown in **Figure 5**. A peak at 742 m/z in spectra allowed for the identification of the chemical moiety C₃₀H₂₄N₈O₈CO₂. The 282, 251, and 212 m/z peaks, which are also distinct, could be attributable to various pieces. The electron impact mass spectrum of the Rh(III) complex is shown in **Figure 6**. The signal at 937 m/z for the complex moiety C₃₀H₂₈Cl₂N₈O₁₀Rh₂ matched this moiety. There are other significant peaks at 350, 319, 149, and 123 m/z that may be due to more fragments. The electron impact mass spectrum of the Rh(III) complex is shown in **Figure 7**. This moiety was represented by a peak at 933 m/z for the complex moiety C₃₀H₂₈Cl₂N₈O₁₀Ru₂. There are other distinct peaks at 349, 318,

149, and 123 m/z that might be due to more fragments. **Schemes 2–5** discuss potential fragmentation paths and the structural tagging of fragments [9].

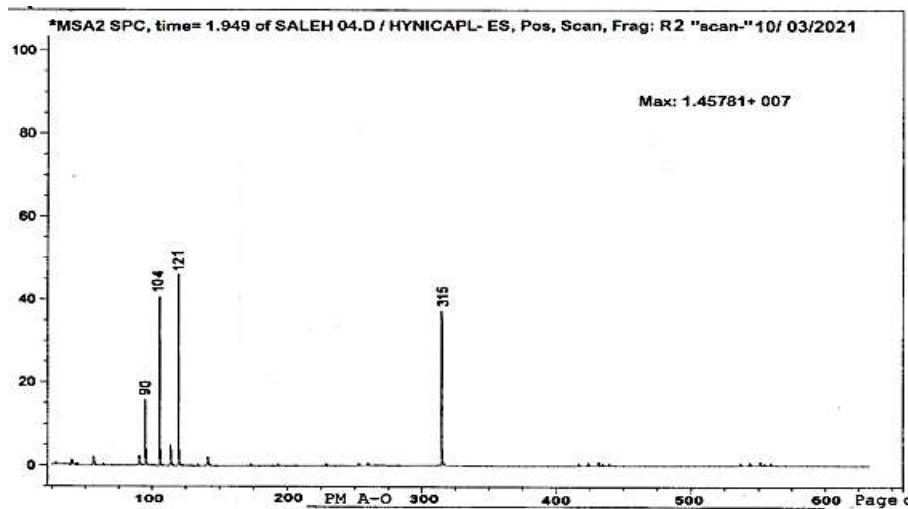


Figure 3. LMS of ligand

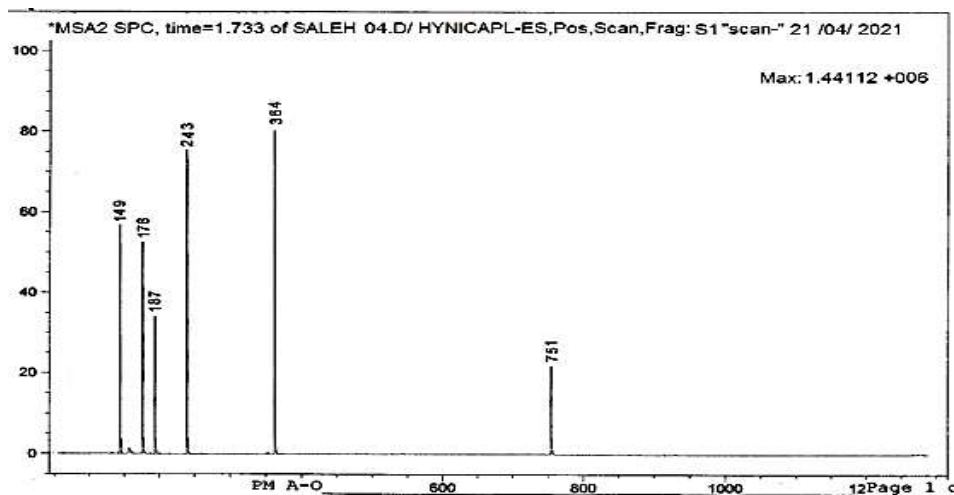


Figure 4. LCMS of Cucomplex

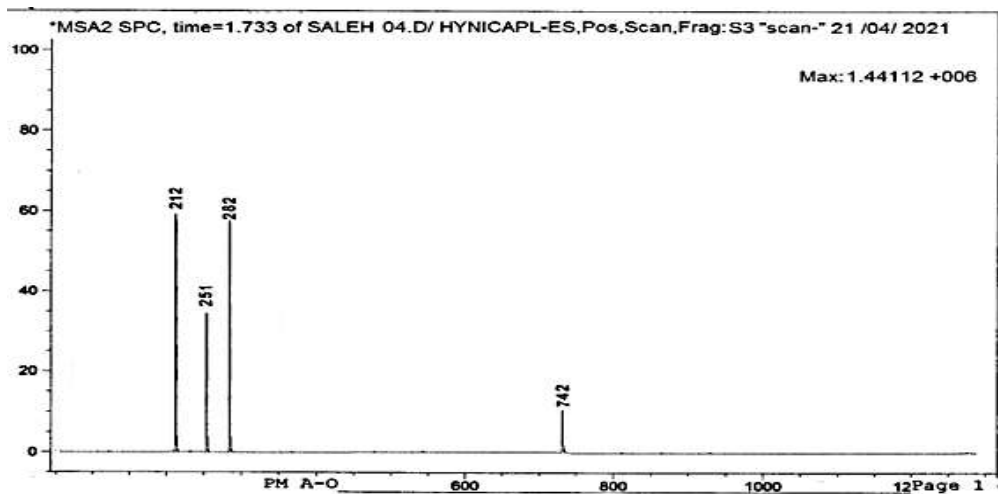


Figure 5. LCMS of Co complex

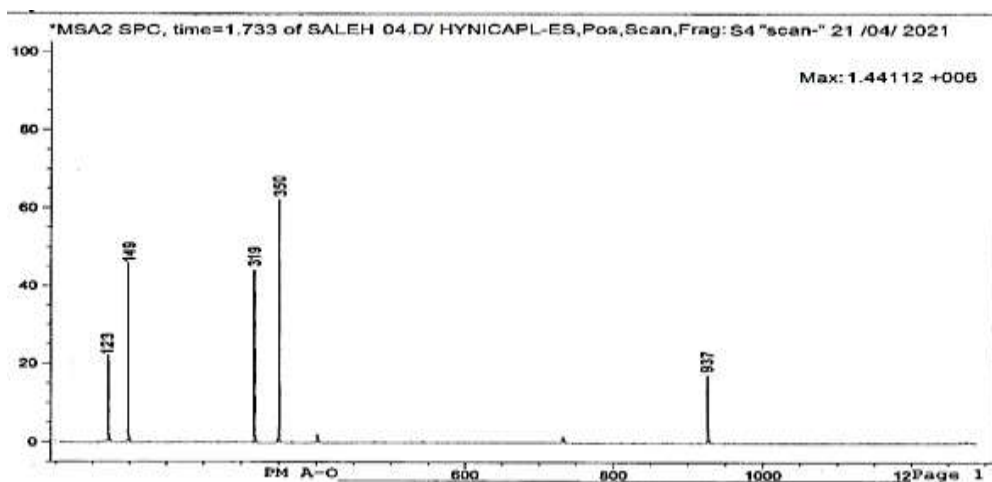


Figure 6. LCMS of Rh complex

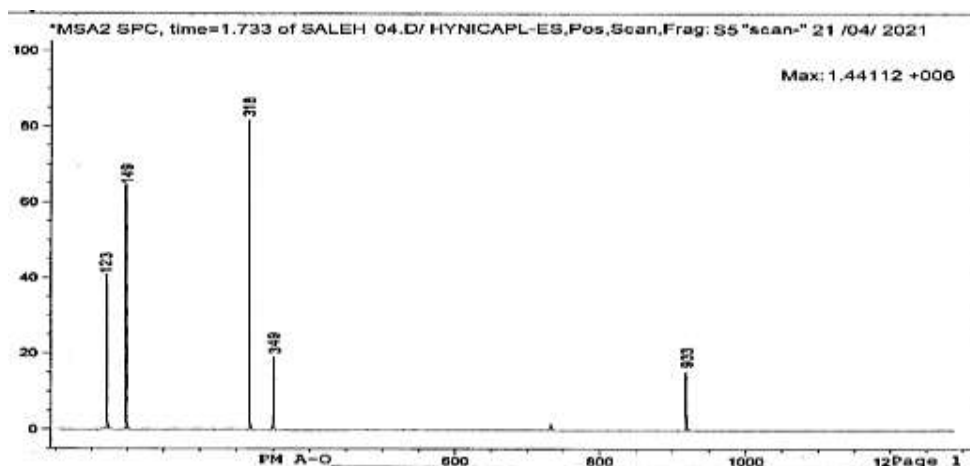
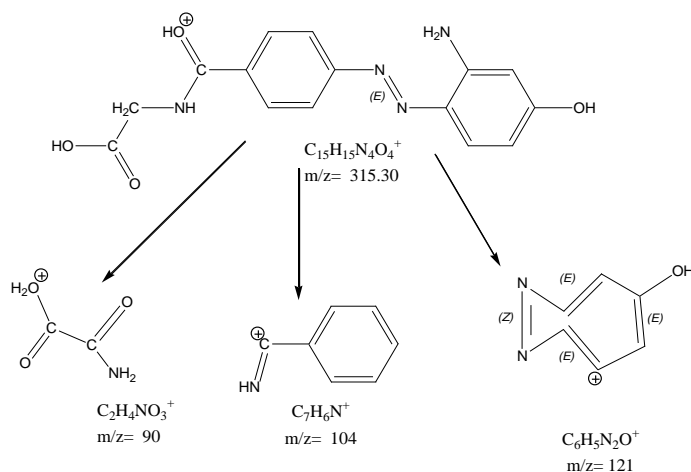
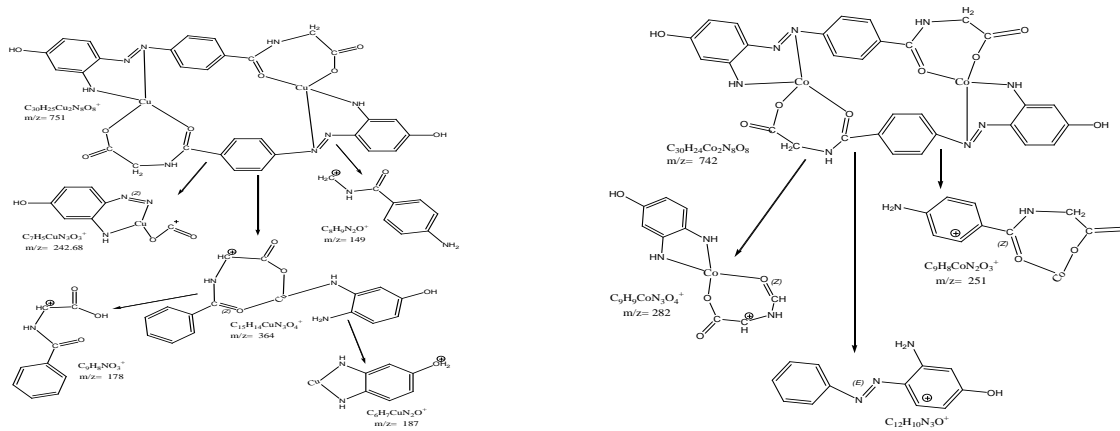


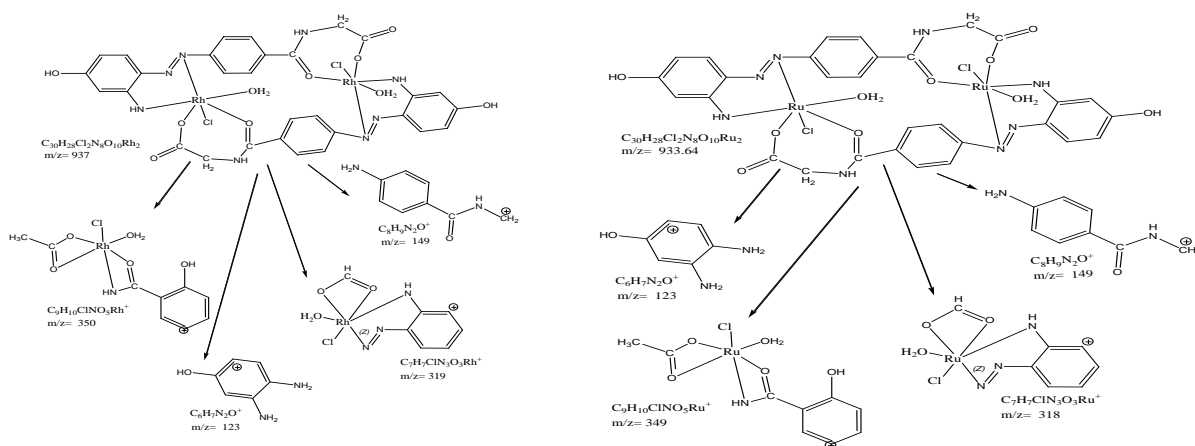
Figure 7. LCMS of Ru complex



Scheme 2. Fragmentation pattern of LH₂



Scheme 3. Fragmentation pattern of Cu(II) complex Scheme 4: Fragmentation pattern of Co(II) complex



Scheme 5. Fragmentation pattern of Rh(III) complex Scheme 6: Fragmentation pattern of Ru(III) complex

3.5. Measurements of Infrared spectra

In order to identify the functional groups in molecules, especially organic molecules, FTIR spectra was used. In some situations, where coordination happens by changing the functional group frequencies (that have the donating atom), this data can provide hints for the formation of complexes. **Table 3** compiles and arranges the spectra of azoligands and their metalchelate

complexes with Cu(II), Co(II), Ru(III), and Rh(III). Bands in the ligand's spectrum at 3421 and 3367 cm^{-1} , which were attributed to the stretching vibration of (NH_2), were reduced to a lower frequency in all generated compounds, indicating coordination with a metal ion [17]. The band located at 1472 cm^{-1} in the unbound azo ligand was given the ($\text{N}=\text{N}$) stretching vibration (LH_2). This band was found in the spectra of the substances between 1454 and 1464 cm^{-1} . It was proven that the azo group was involved in the chelation by the azo group of the azo ligand [18, 19]. Additionally, earlier studies have shown that the azo-dye nitrogen invariably prefers complexation when transition metals are present. [20] It was challenging to prove that this group was involved in chelate formation because the Rh(III) and Ru(III) complexes include coordinated water molecules. The presence of OH bands in the (3381 and 3358) cm^{-1} of the Rh(III) and Ru(III) complexes, respectively, in the IR spectrum was attributed to the existence of coordinated water molecules in the coordination sphere. Additionally, it was discovered that stretching vibrations in the ranges of (833 and 768-770 cm^{-1}) correspond to ν . ($\text{M}-\text{OH}_2$). The IR spectra showed a significant stretching vibration band at 3522 cm^{-1} , which corresponds to the phenolic group's OH, which is a strong indication that water molecules are engaged in the coordination of the unbound ligand. 21 This band did not experience displacement due to a lack of coordination. All complexes' spectra showed band shifts to higher wave numbers for asymmetric stretching vibrations in the range of (1636–1676 cm^{-1}) and lower frequencies for symmetric stretching vibrations assigned to the carboxylate group (COO^-). This suggests that the COO^- anion's oxygen participates in the coordination of the metal ions. The ν values (200) were compatible with carboxylate monodentate coordination behavior, just like in the case of the LI complexes. New bands that only showed in the produced compounds were found when comparing the spectra of all complexes with the free ligand, indicating that the preparation was successful. In the Ru(III) and Rh(III) complexes, three bands were attributed to ($\text{M}-\text{N}$), ($\text{M}-\text{O}$), and ($\text{M}-\text{Cl}$), whereas two bands were attributed to ($\text{M}-\text{N}$) and ($\text{M}-\text{O}$) in the Cu(II) and Co(II) complexes. 18,22,23 Last but not least, it can be deduced from the IR spectra of all produced compounds that the azodye ligand is coupled to the metal ions through four sites (the N site of the azo group, the primary amine, and the O site by deprotonation of the carboxyl and amidic carbonyl) [18, 23, 24]. Therefore, in all of the prior compounds, the ligand displayed N, N, O, and O tetradentate behavior [9, 16, 18, 26, 28, 29–33].

Table 3. list the IR spectra bands of the free azo ligand and complexes (cm^{-1})

Comp.	ν OH phenolic	ν amine	ν amide	ν ($\text{N}=\text{N}$)	ν CO of -CON-H-	ν (CO O ⁻) assy.	ν (CO O ⁻) sym.	ν (H_2O coordinated)	$\Delta\nu$	Other bands
LH_2	3421	-	3266	1454	1622	1541	1387	-	15 4	-
$[\text{Cu}_2\text{L}_2]$	3396	3325	3281	1415	1676	1645	1354	-	29 1	ν MN(565,52 4) ν MO(488,44 7)

[Co ₂ L ₂]	3398	3358	3229	1498	1650	1609	1331	-	27	v	
									8	MN(560,515)	
										v	
										MO(466,424)	
[RuL ₂ Cl ₂ (H ₂ O) ₂]	3439	3142	3258	1440	1736	1641	1352	3358	28	v	
								833	9	MN(563,530)	
								768		v	
										MO(480,442)	
										v	
										MCl(374,341)	
[RhL ₂ Cl ₂ (H ₂ O) ₂]	3348	3283		1442	1651	1609	1333	3381	27	v	
								833	6	MN(542,516)	
								770		v	
										MO(449,472)	
										v	
										MCl(324,345)	

3.6. Thermal measurements

The heat breakdown of the ligand LH₂ and related metal complexes is depicted in **Figures 8, 9, 10, and 11**, as well as the TG and DTG data. Information about the thermal degradation process is provided in **Table 4**. The TG decomposition curve for the produced compounds showed a decomposition, with the ligand's thermal stability being poor at 70 °C, similar to the low stability complexes in the range of (135, 100, 91, and 60 °C) for Cu(II), Co(III), Rh(III), and Ru(III) complexes, respectively. This indicated the presence of water molecules only in the Rh(III) and Ru(III) complexes, whether water. The ligands Cu(II), and Co(II) disintegrate in a single step, leaving an intact residue. The Rh(III) complex breaks down in two steps, leaving behind an intact residue. The Ru(III) complex, however, breaks down in four phases with a complete residue. This is consistent with the computed values and suggested formulas. [35-40]

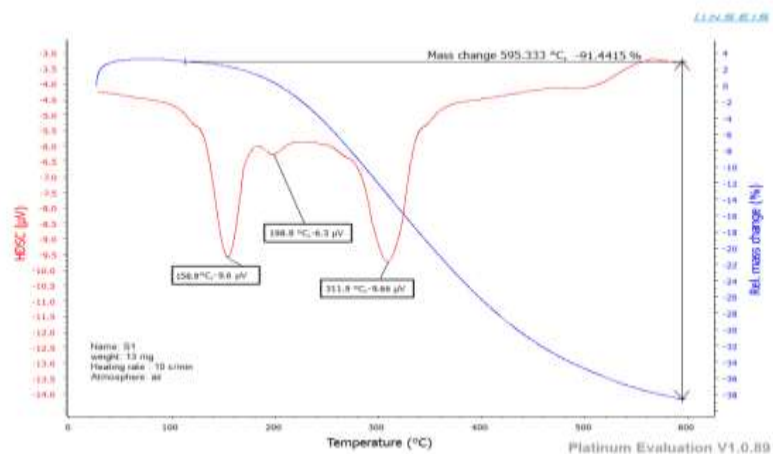


Figure 8. Thermogravimetry of Ligand

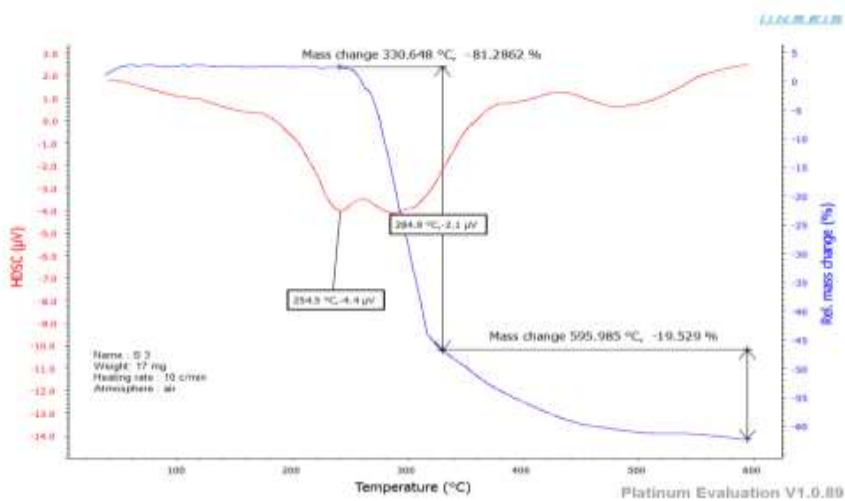


Figure 9. Thermogravimetry of Co complex

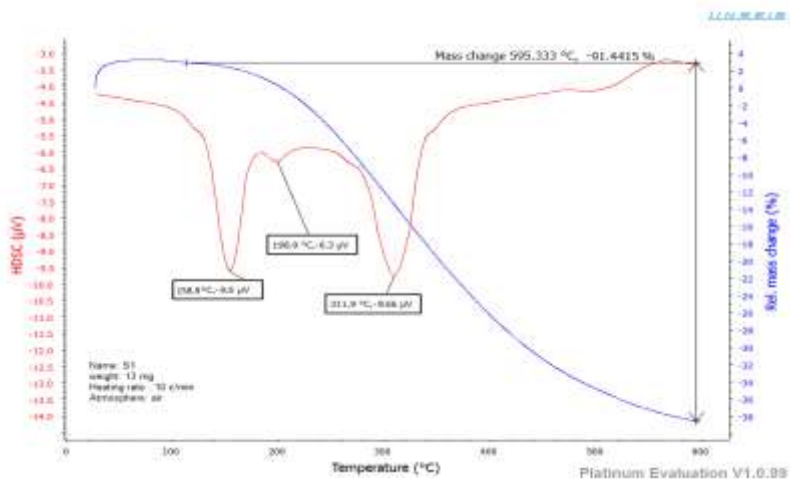


Figure 10. Thermogravimetry and DSC of Cu complex

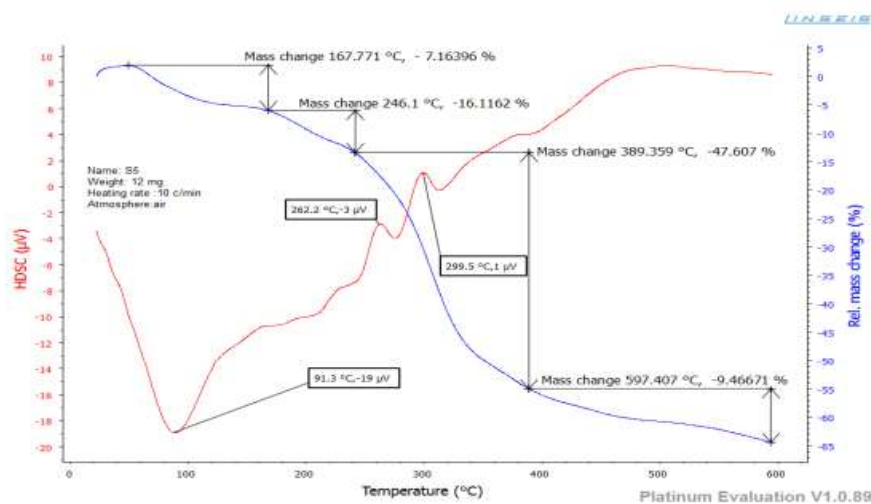


Figure 11. Thermogravimetry of Ru complex

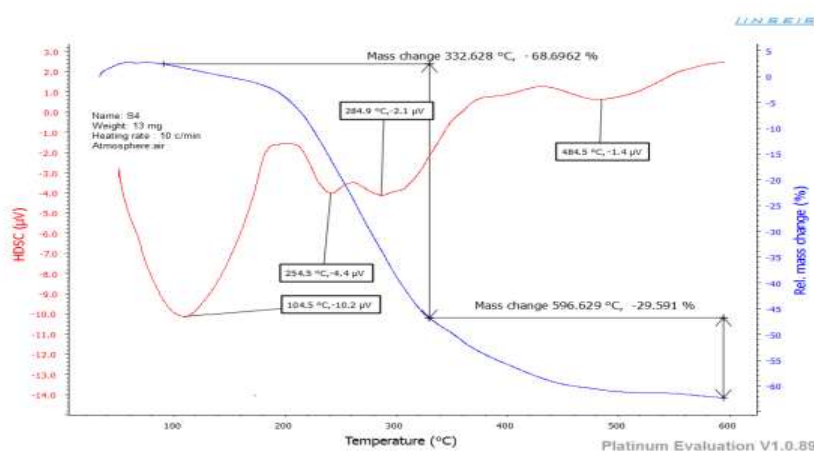


Figure 12. Thermogravimetry of Rh complex

Table 4. Ligand and its complexes undergo thermal degradation

Comp.	(Range of TG) °C	Max of DSC °C	ΔH μV	% Found (calculated)		Assignment
				weight loss	decrease of mass overall	
L ₁	65.38-326.996		-			-
	326.996	114.8(Endo)	13.4	49.4596(49.6815)	95.2139 (96.1783)	CO ₂ , CO, C ₃ H ₆ N ₃
		169.8(Endo)	12.	27.2126(26.1146)		O
	489.227	319(Endo)	2	18.5417(20.3822)		- C ₄ H ₄ NO
	489.227-595.383	473(Endo)	-8.5			- C ₅ H ₄
			-7.5			- ResidueC
[Co ₂ (L ₁) ₂]	100-330	254.5(Endo)	-4.4			
C ₃₀ H ₂₄ Co ₂ N ₈ O ₈	330-438	284.9(Endo)	-2.1	81.29(79.78)	81.29 (79.78)	-C ₃₀ H ₂₄ N ₈ O ₆
	438-593	490 (Endo)	0.5			- Residue 2CoO
[Cu ₂ (L ₁) ₂]	135-595	158.9(Endo)	-9.6	91.545	91.545	-C ₃₀ H ₂₄ N ₈ O ₇ , CuO
C ₃₀ H ₂₄ Cu ₂ N ₈ O ₈		198.9(Endo)	-6.3	(91.4415)	(91.4415)	- Residue Cu

		311.9(Endo)	-				
)	9.6				
		470.0(Exo)	6				
		560.0(Exo)					
[Ru(L ₁) ₂ Cl ₂ (H ₂ O) ₂]	60-165	91.3(Endo)	-19	7.16396(6.855)			-2H ₂ O+CO
C ₃₀ H ₂₈ Cl ₂ Ru ₂ N ₈ O ₁	165-240	262.2(Exo)	-3	16.1162(16.8159)			-C ₂ H ₂ Cl ₂ N ₂ O ₂
	240-385	299.5(Exo)	1		80.35387		- C ₂₄ H ₂₀ N ₆ O ₃
	385-595	380(Endo)	4	47.607(47.127)	(79.8485)		-C ₂ H ₂ , 0.5RuO
				9.46671(9.0506)			- Residue
		104.5(Endo)					1.5RuO
)	10.				
[Rh(L ₁) ₂ Cl ₂ (H ₂ O) ₂]	91-330	254.5(Endo)	2	68.6962(69.0501)			-H ₂ O, CO ₂ , CO,
C ₃₀ H ₂₈ Cl ₂ Rh ₂ N ₈ O ₁	330-595)	-4.4)	68.6962(69.0501)		C ₂₇ H ₁₈ Cl ₂ N ₈ O ₂
		284.9(Endo)	-2.1)		-Residue
)	-1.4				CH ₈ O ₄ Rh ₂
		484.5(Endo)					
)					

4. Conclusion

It's important to know how the compensated groups are spread out in relation to the azo group because there are aromatic rings connected to the nitrogen atoms of the azo group and the compensated groups at different points in the aromatic ring, which can be acidic, basic, or both. As an example, the hydroxyl group attached to the ortho site would be more significant, and this group of compounds includes orthohydroxyazo substances. In this effort, we are synthesizing a brand-new azo ligand. This type of reagent was chosen since it has numerous consistency sites, seven unique chelate compounds with some metallic ions, and can be used to characterize the ligand and its complexes using a variety of techniques. The production of all azo compounds in this work, which concentrated on the synthesis of novel azo compounds, was verified by Fourier transform infrared (FTIR), ¹H-NMR spectrum characterization, and chemical analysis.

References

- Hasan, S.M. Synthesis, Characterization Structure Determination from Power X-Ray Diffraction Data, and Biological Activity of Azodye of 3-Aminopyridine and Its Complexes of Ni(II) AND Cu(II); *Bulletin of the Chemical Society of Ethiopia*, **2020**, *34*, 523-532.
- Ewa, W.W.; Natalia, Ł.; Jan, F.B.; Elżbieta, L. Azo Group(s) in Selected Macrocyclic Compounds, *Journal of Inclusion Phenomena and Macrocyclic Chemistry*, **2018**, *90*, 189–257.
- Said, B.; Souad, M.; El Harfi, A. Classifications, Properties, Recent Synthesis and Applications of Azo Dyes; *Heliyon*, **2020**, *6*, e03271.
- Joseph, K.A.; Cedric, D.K.A.; Nurudeen, M.I. Cynthia, A.D.; Charles, O.A.; Dorcas, D.G.; Joseph, S.A. Synthesis and In Vitro Antimicrobial and Anthelmintic Evaluation of Naphtholic and Phenolic Azo Dyes; *Journal of Tropical Medicine*, **2020**, *2020*, 1-8.
- Yousaf, A.; Shafida, A.H.; Umer, R. Biomedical Applications of Aromatic Azo Compounds; *Mini-Reviews in Medicinal Chemistry*; **2018**, *18*, 1548-1558.

6. El-Sayed, Y.; Mohamed, G.; El-Wakeil, N.; Ahmed, A.; El-Nagar, A. Metal Complexes of Azomesalamine Drug: Synthesis, Characterization, and Their Application as an Inhibitor of Pathogenic Fungi; *Applied Organometallic Chemistry*, **2021**, e6290.
7. Siham, S.; Adeline, F.T.; Gérald, L.; Amina, A.; El-Ghayoury, A. Imidazole and Azo-Based Schiff Bases Ligands as Highly Active Antifungal and Antioxidant Components; *Heteroatom Chemistry*; **2019**, 2019, 1-8.
8. Khalid, J.A.; Khamis, A.A.; Zainab, M.A. Synthesis and Spectroscopic Properties of Some Transition Metal Complexes with New Azo-Dyes Derived From Thiazole and Imidazole; *Asian Journal of Chemistry*; **2013**, 25,10475-10481.
9. Al Zoubi, W.; Vian, Y.J.; Veyan, T.S.; Al-Hamdani, A.A.S.; Suzan, D.A. Synthesis and Bioactivity Studies of Novel Schiff Bases and Their Complexes; *Journal of Physical Organic Chemistry*. **2019**, e4004,1-7.
10. Wannas N.M.; Al-Hamdani A.A.S.; Al-Zoubi W. Spectroscopic Characterization for New Complexes with 2,2'-(5,5-Dimethylcyclohexane-1,3-Diylidene)bis(azan-1-yl-1-Ylidene)Dibenzoic acid; *Journal of Physical Organic Chemistry*, **2020**, 33,1-12.
11. Al-Hamdani, A.A.S.; Balkhi, A.M.; Falah, A. Synthesis, Spectroscopic and Biological Activity Studies of Azo-Schiff Base and Metal Complexes derived from 5-Methyltryptamine; *Damascus University Journal for Basic sciences*, **2013**, 29,21-41.
12. Reem, G.D.; Walaa, H.M.; Gehad, G.M. Metal complexes of tetradentateazo-dye ligand derived from 4,40-oxydianiline: Preparation, structural investigation biological evaluation and MOE studies; *Applied Organometallic Chemistry*; **2020**, e5883:1-20.
13. Reem, A.; Ismail, A.; Amerah, A.; Khlood, S.A.; Abdulmajeed, F.A. et al. Synthesis and Characterization for New Mn(II) Complexes; Conductometry, DFT, Antioxidant Activity via Enhancing Superoxide Dismutase Enzymes that Confirmed by in-Silico and in-Vitro Ways; *Journal of Molecular Structure*; **2021**,1243,1-14.
14. Manika, R.; Chavan, V.L. Thermal and Antimicrobial Studies of Synthesized and Characterized Rhodium, Platinum and Gold Metal Complexes Derived from (2E) N-(naphthalen-2yl)-3 phenyl prop-2en-1 imine Schiff Base, *Journal of Social Sciences*. **2021**, 65,30-38.
15. Ahmed, N.A. Synthesis, Characterization and Microbicides Activities of N-(hydroxy-4-((4-nitrophenyl)diazenyl)benzylidene)-2-(phenylamino)Acetohydrazide Metal Complexes. *Egyptian Journal of Chemistry*; **2020**, 63,1509-1525.
16. Vian, Y.J.; Veyan, T.S.; AL-Hhamdani, A.A.S.; Suzan, D.A. Preparation, Spectroscopic Characterization and Theoretical Studies of Transition Metal Complexes with 1-[(2-(1H-indol-3-yl)ethylimino)methyl]naphthalene-2-ol Ligand; *Chemistry An Asian Journal*. **2019**, 31,2430-2438.
17. Suleman, V.T.; Al-Hamdani, A.A.S.; Ahmed, S.D.; Jirjees, V.Y.; Khan M.E. et al.; Phosphorus Schiff base ligand and its complexes: Experimental and theoretical investigations; *Applied Organometallic Chemistry*; **2020**, 34(4),1-16.
18. Nakamoto, K. Infrared and Raman Spectra of Inorganic and Coordination Compounds, Wiley-Inter Science: New York. **1997**.
19. Kareem, M.J.; Al-Hamdani, A.A.S.; Ko, Y.G.; Al Zoubi, W.; Mohammed, S.G. Synthesis, Characterization, and Determination Antioxidant Activities for New Schiff Base Complexes Derived from 2-(1H-indol-3-yl)-ethylamine and Metal Ion Complexes; *Journal of Molecular Structure*; **2021**,1231,1-30.

20. Obaid, S.M.H.; Sultan, J.S.; Al-Hamdani, A.A.S. Synthesis, Characterization and Biological Efficacies from Some New Dinuclear Metal Complexes for Base 3-(3, 4-Dihydroxy-phenyl)-2-[(2-hydroxy-3-methylperoxy-benzylidene)-amino]-2-methyl Propionic Acid; *Indonesian Journal of Chemistry*, **2020**, 20, 1311-1322.
21. Al-Hamdani, A.A.S.; Al Zoubi, W. New Metal Complexes of N₃ Tridentate Ligand: Synthesis, Spectral Studies and Biological Activity; *Spectrochimica Acta Part A: Molecular and Biomolecular Spectroscopy* **2015**, 137, 75-89.
22. Al-Hamdani, A.A.S.; Hasan, Z.A.A. Spectroscopic Studies and Thermal Analysis of New Azo Dyes Ligands and their Complexes with Some Transition of Metal Ions. *Baghdad Science Journal*, **2016**, 13, 511-523.
23. Al Zoubi, W.; Al-Hamdani, A.A.S.; Ahmed, S.D.; Basheer, H.M.; Al-Luhaibi, R.S.; Dib, A.; Ko, Y.G. Synthesis, Characterization, and Antioxidant Activities of Imine Compounds. *Journal of Physical Organic Chemistry*, **2018**, 32, 1-9.
24. Lever, A.B.P. Inorganic Electronic Spectroscopy, *Elsevier Publishing Company: Amsterdam, London*, **1968**, 121, edn6.
25. Jirjees, V.Y.; Suleman, V.T.; Al-Hamdani, A.A.S.; Ahmed, S.D. Preparation, Spectroscopic Characterization and Theoretical Studies of Transition Metal Complexes with 1-[(2-(1H-indol-3-yl)ethylimino)methyl]naphthalene-2-ol Ligand. *Chemistry An Asian Journal*, **2019**, 31, 2430- 2438.
26. Kareem, M.J.; Al-Hamdani, A.A.S.; Ko, Y.G.; Al Zoubi, W.; Mohammed, S.G. Synthesis, Characterization, and Determination Antioxidant Activities for New Schiff Base Complexes Derived from 2-(1H-indol-3-yl)-ethylamine and Metal Ion Complexes. *Journal of Molecular Structure*, **2021**, 1231, 1-30.
27. Obaid, S.M.H.; Sultan, J.S.; Al-Hamdani, A.A.S. Synthesis, Characterization and Biological Efficacies from Some New Dinuclear Metal Complexes for Base 3-(3, 4 Dihydroxy-phenyl)-2-[(2-hydroxy-3-methylperoxy-benzylidene)-amino]-2-methyl Propionic Acid. *Indonesian Journal of Chemistry*, **2020**, 20, 1311-1322.
28. Al-Hamdani, A.A.S.; Al-Khafaji, N.R.; Shaalan. N. Preparation, Spectral, Thermal and Bio Activity Studies of Azo Dyes Complexes. *Research journal of pharmaceutical biological and chemical sciences*. **2017**, 8, 740-750.
29. Al Zoubi, W.; Kim, M. J.; Al-Hamdani, A.A.S.; Kim, Y.G.; Ko, Y.G. Phosphorus-Based Schiff Bases and Their Complexes as Nontoxic Antioxidants: Structure–Activity Relationship and Mechanism of Action. *Applied Organometallic Chemistry*, **2019**, 33, 1-16.
30. Jirjees, V.Y.; Al-Hamdani, A.A.S.; Wannas, N.M.; Faeqad, A.R.; Dib, A.; Al Zoubi, W. Spectroscopic Characterization for New Model from Schiff Base and Its Complexes. *Journal of Physical Organic Chemistry*, **2020**, 2020, 1-16.
31. Al-Daffay, R.K.H.; Al-Hamdani, A.A.S. Synthesis and Characterization of Some Metals Complexes with New Acidicazo Ligand 4-[(2-Amino-4-Phenylazo)-Methyl]-Cyclohexane Carboxylic Acid; *Iraqi Journal of Science*; **2022**, 63, 3264-3275.
32. Samy, M.E.; Moamen, S.R.; Fawziah, A.A.; Reham, Z.H. Situ Neutral System Synthesis, Spectroscopic, and Biological Interpretations of Magnesium(II), Calcium(II), Chromium(III), Zinc(II), Copper(II) and Selenium(IV) Sitagliptin Complexes; *International Journal of Environmental Research and Public Health*; **2021**, 18, 1-19.
33. Kirill, V.Y.; Aleksandr, S.S.; Werner, K.; Sergey, A.G. Synthesis and Crystal Chemistry of Octahedral Rhodium(III) Chloroamines. *Molecules*, **2020**, 25, 1-17.

34. Kareem, M.J.; Al-Hamdani, A.A.S.; Jirjees, V.Y.; Khan, M.E.; Allaf, A.W. ;Al Zoubi, W. Preparation, Spectroscopic Study of Schiff Base Derived from Dopamine and Metal Ni (II), Pd (II), and Pt (IV) complexes, and activity determination as antioxidants. *Journal of Physical Organic Chemistry*, **2020**, 34,1-15.
35. Al Zoubi, W.; Al-Hamdani, A.A.S.; Ko, Y.G. Schiff Bases and Their Complexes: Recent Progress in Thermal Analysis. *Sep Sci Technol.*, **2017**, 52,1052-1069.
36. Al-Daffay, R.K.H. Preparation-and Spectroscopic Characterization of Transition Metal Complexes with Schiff base 2-[1-(1*H*-indol-3-yl)ethylimino) methyl] naphthalene-1-ol , *Baghdad Science Journal* ,**2022**; 2022,1036-1044.
37. Al-Khazraji, A.M.A.; Al Hassani, R.A.M. Synthesis, Characterization and Spectroscopic Study of New Metal Complexes form Heterocyclic Compounds for Photostability Study. *Systematic Reviews in Pharmacy*, **2020**, 11,535-555.
38. Reem, G.D.; Walaa, H.M.; Gehad, G.M. Metal Complexes of Tetradentateazo-Dye Ligand Derived from 4,4-Oxydianiline: Preparation, Structural Investigation, Biological Evaluation and MOE Studies. *Applied Organometallic Chemistry*, **2020**, 34,1-20.
39. Al-Daffay, R.K.H.; Al-Hamdani, A.A.S. Synthesis, Characterization, and Thermal Analysis of a New Acidicazo Ligand's Metal Complexes. *Baghdad Science Journal*, **2022**, 2022,121-133.
40. Al-Daffay, R.K.H.; Al-Hamdani, A.A.S. Synthesis, Characterization and Thermal Analysis of Cr(III), Mn(II) and Zn(II)Complexes of a New Acidicazo Ligand. *Chemical Methodologies*, **2022**, 6,507-521.
41. Al-Hamdani, A.A.S, Al-Alwany, T.A.M.; Mseer, M.A.; Fadhel, A.M.; Al-Khafaji, Y.F. Synthesis, Characterization, Spectroscopic, Thermal and Biological Studies for New Complexes with N1, N2-bis (3-hydroxyphenyl) Oxalamide. *EgyptJ. of Chem.***2023**,66,223-235.